analytical chemistry

pubs.acs.org/ac Article

A Chimeric Photo-Controllable CRISPR/Cas12a System for Universal and Fast Diagnostics

Xinrong Yan, Bin Liu, Shuguang Zhou, Yanjun Fan, Shijiong Wei, Dehui Qiu, Henglong Xiang, Jiahang Zhou, Jean-Louis Mergny, David Monchaud, Huangxian Ju, and Jun Zhou*

Cite This: *Anal. Chem.* 2025, 97, 24634−24642 Read Online

ACCESS | Metrics & More | Article Recommendations | Supporting Information

ABSTRACT: The potential of clustered regularly interspaced short palindromic repeats (CRISPR) and corresponding CRISPR-associated (Cas) protein systems (CRISPR/Cas) systems for biomedical applications is tremendous; however, precise control of their activity is essential to better harness this potential and, beyond this, to develop reliable diagnostic reagents. Herein, we report on such a strategy by controlling the CRISPR/Cas12a activity using a photo-controllable CRISPR RNA (crRNA). To this end, the 3′ end of crRNA was conjugated to a G-quadruplex (G4) block through a photocleavable linker: upon photo irradiation, the G4 trigger is removed, thus allowing for the DNA target to access and hybridize with the crRNA, and thus be processed by the CRISPR/Cas12a system. The efficiency of this approach was demonstrated by the detection of human papillomavirus 16 DNA in 50 clinical samples: our one-pot strategy was found to be as efficient as the routinely implemented method (qPCR), with 95.7% sensitivity and 100% specificity, in addition to be faster (25 versus 60 min) and both simpler and less expensive (being implementable as lateral flow test strips). Collectively, this new and fully controllable CRISPR/Cas system holds great potential for next-generation clinical diagnostics.

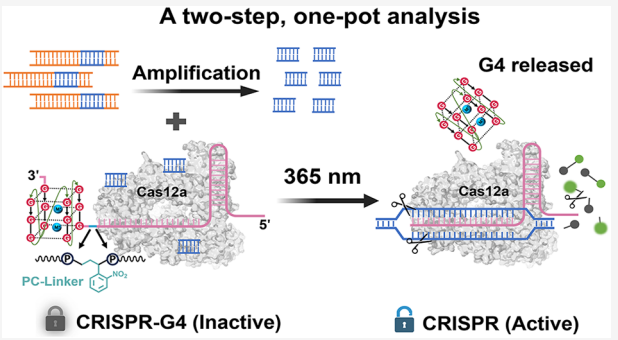

INTRODUCTION

The clustered regularly interspaced short palindromic repeats (CRISPR) and corresponding CRISPR-associated (Cas) protein systems (CRISPR/Cas) are powerful tools for gene editing and molecular diagnostics.[1,2] CRISPR systems are categorized into two classes, that is, class 1 and class 2. The class 1 systems utilize multiprotein effector complexes to recognize and degrade target DNA. The CRISPR-Cas3 system, a key member of this class, features a core Cas3 protein with nonspecific nuclease activity against single-stranded DNA (ssDNA). This unique trait makes it a highly promising candidate for nucleic acid diagnostics. Despite the developmental challenges posed by their numerous components, bulky size, and inherent complexity, the distinctive mechanisms of class 1 systems still offer valuable frameworks for advancing novel molecular diagnostics.[3−5] For class 2 CRISPR systems, they rely on the enzymatic properties of a single-effector protein (being either Cas9, Cas12, Cas13, or Cas14), which display subtle differences in activity: for instance, Cas9 creates blunt double-stranded DNA (dsDNA) breaks, while Cas12 creates staggered DNA cuts.[6−9] Both Cas12a and Cas12b have been used for gene editing: as above, they display subtle differences, as Cas12a is associated with a single RNA guide (vide infra), while Cas12b is a dual-RNA-guided endonuclease. However, CRISPR/Cas12a is far more widely used than CRISPR/Cas12b, the former being discovered before the latter (2015 versus 2019).[7,10] Cas12a associates with CRISPR RNA (crRNA) to form a ribonucleoprotein (RNP) complex that possesses a dual catalytic function, i.e., both target-dependent *cis*-cleavage and nonspecific ssDNA *trans*-cleavage.[11,12] Given the high enzymatic activity and high specificity of Cas12a, the corresponding CRISPR/Cas12a system is currently being widely used, notably for nucleic acid diagnostics.[13−15] However, this system is not sensitive enough[16,17] to circumvent a nucleic acid amplification (NAA) step before CRISPR detection.[18] More importantly, the NAA step is not compatible with that of CRISPR, which leads to perform the two steps separately, at the expense of aerosol contamination risks.[19−21]

Strategies to improve the use of CRISPR/Cas12a system were recently developed,[22,23] notably via crRNA engineering that allows for controlling CRISPR activity.[24,25] For example, using a photocleavable blocking strand, complementary to the

Received: August 5, 2025
Revised: October 16, 2025
Accepted: October 17, 2025
Published: October 30, 2025

https://doi.org/10.1021/acs.analchem.5c04782
Anal. Chem. 2025, 97, 24634−24642

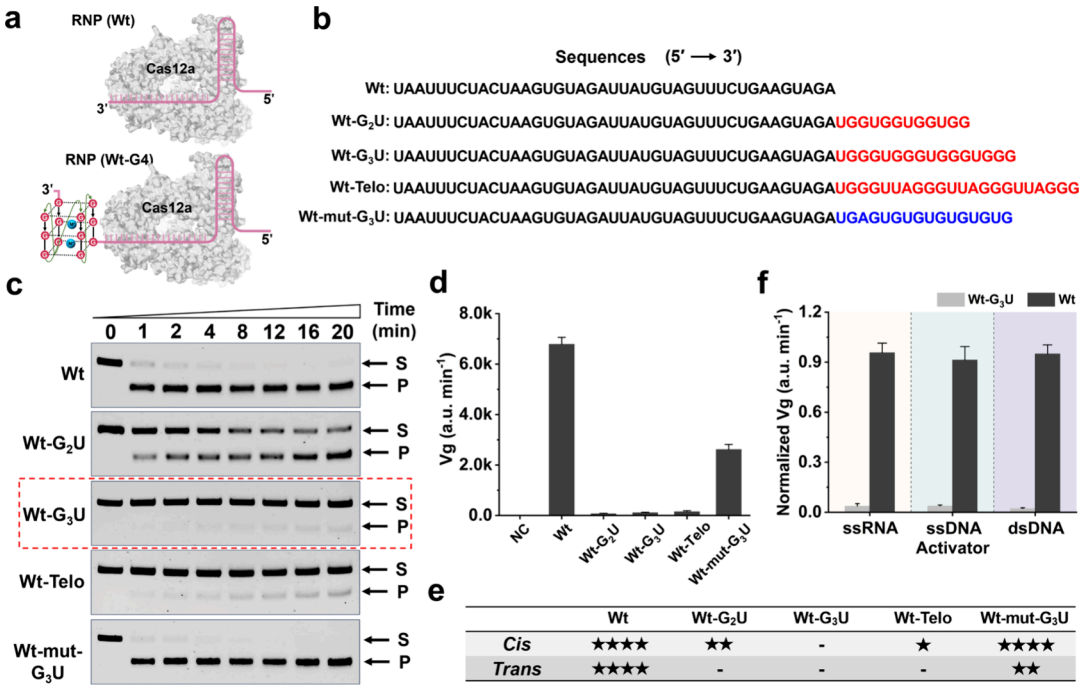

Figure 1. Chimeric crRNA-G4s inhibit the *cis*- and *trans*-cleavage activities of Cas12a. (a) Schematic of the RNP formed by wild-type crRNA (Wt) or chimeric crRNA-G4 (Wt-G4) with Cas12a. (b) Sequences of the crRNAs used in the study of Cas12a cleavage events, the red and blue parts represent the sequences that can and cannot form G4, respectively. (c) Time-dependent *cis*-cleavage of substrate by Cas12a in the presence of different crRNA-G4s. The concentrations of the dsDNA substrate and RNP are 5 and 65 nM, respectively. The "S" and "P" bands indicate the substrate and *cis*-cleavage product, respectively. The raw data are shown in Figure S3. (d) Evaluation of the *trans*-cleavage activity of Cas12a with different crRNA-G4s. The concentration of the ssDNA target is 1 nM and the RNP is 10 nM. "Vg" represents the reaction rate, which is calculated from the slope of the fluorescence curve in the first 5 min. The raw data are shown in Figure S4. (e) Summary of the effect of crRNA-G4s on the *cis*- and *trans*-cleavage activities of Cas12a. The "star" corresponds to the cleavage activity (more stars, higher activity), whereas "−" signifies that the activity is almost fully inhibited. (f) *Trans*-cleavage reaction rates of Cas12a with different activators ("Vg" is normalized). The concentrations of the activators and RNP are 1 and 10 nM, respectively. The raw data are shown in Figure S5. Data for (d) and (f) are presented as mean ± standard deviation (n = 3 technical replicates).

crRNA, can prevent its binding to the target DNA and thus inactivate the CRISPR system; the resulting CRISPR/Cas could thus be activated by light.[26,27] Another strategy involves the introduction of photolabile groups either on the 2′−OH of the ribose,[28,29] the phosphate backbone,[30] or the nucleotide bases of crRNA through solid-phase synthesis:[31−33] these groups can directly disrupt the interactions between crRNA and either Cas proteins or target DNA, making the corresponding CRISPR/Cas12a system photoactivatable. The use of these light activation-based strategies resolves the incompatibility between NAA and CRISPR detection, making the whole process possible in a one-pot format.[21]

Besides crRNA engineering strategies, CRISPR activity could also be tailored to make it compatible with NAA: for instance, crRNAs targeting substrates with suboptimal protospacer adjacent motifs could reduce the kinetics of Cas12a cleavage, thereby favoring amplicon accumulation and improving detection sensitivity.[34] Moreover, Yu and co-workers found that sodium heparin binds to Cas12a through electrostatic interactions, consequently regulating the activity of the corresponding CRISPR/Cas12a system.[35] Although these strategies can indeed enhance the diagnostic performance of CRISPR-based sensing platforms, their practical convenience is still poor and their generality remains to be proven.

To develop simpler and more universal CRISPR/Cas12a systems, we decided to combine them with G-quadruplex (G4) RNA.[36−39] Indeed, recent studies have shown that G4 can regulate CRISPR activity efficiently; this was achieved in the presence of a G4 ligand that induces the formation and stabilizes the G4 structure, thereby disrupting the function of the guide RNA.[40−42] However, the inherent genotoxicity and possible off-target effects of G4 ligands limit their widespread use, notably for diagnostics applications.[43,44] We reasoned that the promising G4 regulatory concept may be better exploited to regulate CRISPR/Cas12a activity in a more efficient manner. To this end, and on the basis of the crystal structure of the Cas12a-crRNA complex,[45] we hypothesized that the presence of G4 structure in the 3′ region of crRNA may inhibit CRISPR activity without the need of G4 ligand. If feasible, then a novel and more universal CRISPR regulatory strategy could be devised.

We report herein on such a strategy, using a photocontrolled CRISPR/Cas12a system embedding a chimeric, photocleavable crRNA-G4. Our results indicate that the presence of the G4 simultaneously inhibits the *cis*- and *trans*-cleavage activities of Cas12a (Figure 1), and that its inhibitory effect can be removed through photoirradiation. We thus developed a novel G4-based, one-pot CRISPR diagnostic platform by integrating the photocontrolled CRISPR system with a recombinase polymerase amplification (RPA) step. This one-pot assay is user-friendly, avoids contamination issues, and can be spatiotemporally controlled (being ignited by UV light); more importantly, it achieves a sensitivity and specificity comparable to the classically used qPCR detection, making it suited for clinical use.

https://doi.org/10.1021/acs.analchem.5c04782
Anal. Chem. 2025, 97, 24634−24642

EXPERIMENTAL SECTION

Materials and Reagents. DNA sequences, HPV-16 pseudovirus, and ribonuclease R (RNase R) were purchased from Sangon Biotech Co., Ltd. (Shanghai, China). Cas12a was purchased from New England Biolabs (MA, USA). All RNA sequences were supplied by GenScript Biotech Ltd. (Nanjing, China). GelRed (10,000×) was purchased from Biotium Inc. (CA, USA). DNA and RNA loading buffer, RNase inhibitor, RNase-free water, and PrimeSTAR DNA polymerase were purchased from Takara Biotechnology Co., Ltd. (Dalian, China). qPCR mix (High ROX), DNA purification kit, and virus extraction kit were obtained from Vazyme Biotech Co., Ltd. (Nanjing, China). The RPA isothermal amplification kit and lateral flow test strip were purchased from Amp-future Biotech (Changzhou, China). All other reagents and materials, unless indicated otherwise, were of analytical grade and were not further purified.

***Cis*-Cleavage of dsDNA Substrate by Cas12a.** For in vitro cleavage of the dsDNA substrate, the RNP complex was first prepared by incubating equal amounts of Cas12a and crRNA in 1 × Cas12a reaction buffer for 20 min (37 °C). The cleavage system included 5−8 nM of dsDNA substrate and 65 nM of RNP, and the reaction was terminated by adding 1 μL of 20 mg/mL proteinase K after incubation at different time points. The cleavage products were analyzed by 1% agarose gel (containing 1 × GelRed) and imaged with Gel Doc XR+ imaging system (Bio-Rad, USA). ImageJ software was used to quantify the intensity of each band. The cleavage efficiency was calculated using the formula (1):[26]

$$\text{Cleavage eff.} = \left(1 - \sqrt{1 - \frac{b + c}{a + b + c}}\right) \times 100\% \quad (1)$$

where "a" was the intensity of the uncleaved DNA bands, "b" and "c" were the intensities of the cleavage product bands.

Evaluation of the *Trans*-Cleavage Activity of Cas12a. The *trans*-cleavage activity of Cas12a was determined by cleaving the nonspecific ssDNA substrate (F-Q reporter, see Table S2). The 10 μL reaction system contained 1 × Cas12a reaction buffer (50 mM NaCl, 10 mM Tris-HCl, 10 mM $MgCl_2$, 10 mM KCl, 100 μg/mL recombinant albumin, pH 7.9), 10 nM RNP, 500 nM F-Q reporter, and 4 U RNase inhibitor. The mixture was incubated at 37 °C for 30 min, and fluorescence values were collected every 10 s by the StepOnePlus real-time fluorescence system (Applied Biosystems, USA). The *trans*-cleavage reaction rate (Vg) of Cas12a was evaluated by calculating the slope of the real-time fluorescence curve during the first 5 min.

Traditional One-Pot RPA-CRISPR Assay. The traditional one-pot RPA-CRISPR system consists of three components: A, B, and C. Component A (9.5 μL) included 5.9 μL of RPA reagent, 0.4 μL each of forward and reverse primers (10 μM), 0.8 μL of RNase-free water, and 2 μL of DNA template. Ten μL of component B included 1 × Cas12a reaction buffer, 1 μM F-Q reporter, 100 nM RNP, and 8 U RNase inhibitor. Component C was 0.5 μL of 280 mM MgOAc. Finally, components A and B were transferred successively to the bottom of the tube, and then, component C was added and mixed. The tube was incubated at 37 °C for 80 min, and fluorescence signals were collected every 1 min.

Two-Step RPA-CRISPR Assay. In the two-step RPA-CRISPR assay, NAA was first performed via RPA, and then, the amplification products were detected by the CRISPR/Cas12a system. The 10 μL RPA reaction mixture included 5.9 μL RPA reagent, 400 nM of each forward and reverse primer, and 14 mM MgOAc. Subsequently, the mixture was incubated at 37 °C for 20 min, in which 2 μL of RPA product was used in the detection system. The CRISPR detection system consisted of 1 × Cas12a reaction buffer, 50 nM RNP, 500 nM F-Q reporter, 4 U of RNase inhibitor, and 2 μL of RPA product. Next, the mixture was incubated at 37 °C for 60 min, with fluorescence signals collected every 1 min.

Photoinitiated One-Pot CRISPR Assay. Similar to the traditional one-pot RPA-CRISPR method, the proposed photoactivated assay also involved components A, B, and C. The difference here was that the crRNA used in the RNP was Wt-PC-G4 instead of the Wt (Table S1). Components A, B, and C were mixed as described in the traditional one-pot assay, but the reaction was paused after 20 min of incubation at 37 °C. The tube was irradiated using a UV lamp (365 nm, 40 W) for 1 min. This was followed by incubation at 37 °C for 60 min, during which fluorescence signals were collected every 1 min.

Detection of HPV Pseudoviruses with Lateral Flow Test Strips. Nucleic acids from various concentrations of HPV-16 pseudoviruses were extracted using a virus extraction kit and subsequently detected by the proposed method (F-Q reporter was replaced by 1 μM F-B reporter, Table S2). The light-started one-pot CRISPR assay was performed at 37 °C for 20 min, followed by 1 min of UV irradiation and a further 30 min of incubation. Following this, the test strips were inserted into the reaction tubes and kept for 5 min, and the results were imaged via a smartphone.

Ribonuclease Digestion Assay. The 10 μL digestion system included 1 × reaction buffer (20 mM Tris-HCl, 100 mM KCl, and 0.1 mM $MgCl_2$, pH 8.0), 1 μM RNA sample, and 5 U of RNase R. The solution was incubated at 37 °C for different time points and heated at 70 °C for 10 min to terminate the reaction. The digestion results were analyzed using 10% native PAGE.

RESULTS AND DISCUSSION

Construction and Characteristics of Chimeric CRISPR-G4 System. We first validated the role that G4 in crRNA plays in regulating the activity of Cas12a. The formation of G4 in the 3′ region of crRNA was confirmed by circular dichroism (CD) and the G4-specific fluorescent ligand, thioflavin T (Figures S1 and S2). Next, the comparison of the *cis*-cleavage of a dsDNA substrate by the wild-type crRNA (Wt) versus crRNA-G4 (or Wt-G4, Figures 1, S3 and Table S1) revealed that this activity is decreased (G_2U, Telo) or totally abolished (G_3U) in the presence of G4s. This inhibitory property could be reverted using a mutated G4 sequence (mut-G_3U), which is unable to form the G4 structure. Next, the *trans*-cleavage of a fluorophore quencher (FQ)-labeled ssDNA reporter mediated by Wt versus Wt-G4 (Figures 1d, S4 and Table S2), indicated that this activity is completely inhibited by the presence of G4s, the most efficient G4 blocker being G_3U.

We found that the inhibition of Cas12a activity by Wt-G_3U was activator-type independent, as it exhibited nearly complete inhibitory against ssDNA, dsDNA, and ssRNA activators (Figures 1f and S5). To further assess its universal characterization, four different crRNA-G_3U were designed (Figures S6−S8, Table S3): all constructs inhibit both *cis*- and *trans*-cleavage activities of Cas12a, suggesting that this stable G4 could be

https://doi.org/10.1021/acs.analchem.5c04782
Anal. Chem. 2025, 97, 24634−24642

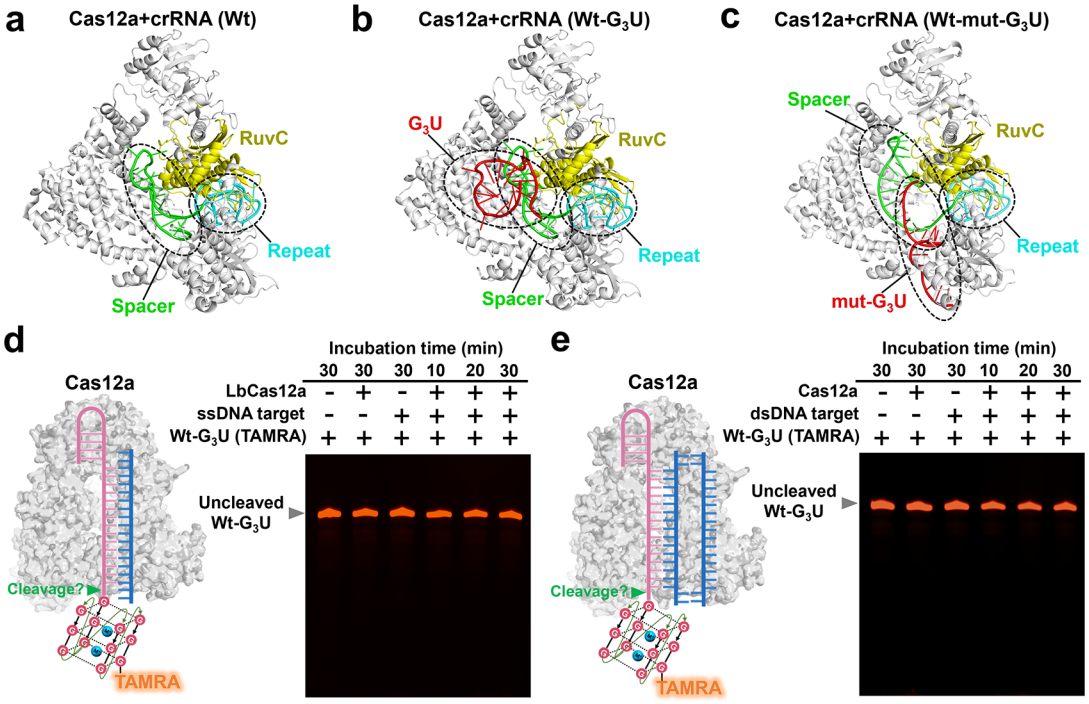

Figure 2. Potential mechanisms of the inhibition of Cas12a activity by chimeric crRNA-G4. (a–c) Results of molecular docking simulations of Cas12a with Wt (a), Wt-G_3U (b), and Wt-mut-G_3U (c). The cyan, green, red, and yellow sections of the crRNA represent the repeat region that interacts with Cas12a, the spacer region that binds to the target, the extension sequences in the 3′ region of the crRNA (where the G_3U or mut-G_3U is present), and the nuclease structural domain of Cas12a, respectively. (d, e) Evaluation of Cas12a-mediated crRNA processing via ssDNA and dsDNA binding, respectively. The results of crRNA processing are analyzed by 20% denaturing PAGE, with both the RNP and target DNA at a concentration of 100 nM.

considered as a universal blocker for controlling CRISPR/Cas12a activity.

Mechanism of Chimeric CRISPR-G4 System. To understand the mechanism by which crRNA-G4 inhibits Cas12a activity, molecular docking simulations were performed using Cas12a in interaction with Wt, Wt-G_3U, or Wt-mut-G_3U. The parallel structure of G_3U G4, predicted by AlphaFold 3,[46] is consistent with the known favored parallel topology of RNA G4s.[47,48] Molecular docking was based on the crystal structure of Cas12a (PDB ID: 8Y03)[45] with the AlphaFold 3-predicted structures of Wt, Wt-G_3U, and Wt-mut-G_3U.

The results seen in Figure 2 showed that the binding of Wt-G_3U and Wt-mut-G_3U to Cas12a was not significantly altered compared with Wt, indicating that the presence of a G4 does not affect the crRNA/Cas12a interaction. However, the presence of the G4 might prevent access of the substrate to the protein channel of Cas12a (Figure 2b); as a consequence, the interaction between the substrate DNA and crRNA might be inhibited by the G4, thus leaving the corresponding CRISPR/Cas12a system inactive.[12] However, mutated G4 should allow the DNA substrate to enter the cleft (Figure 2c). We also speculate that the G4 makes it difficult to be processed by Cas12a in the presence of target DNA.[45] To test this hypothesis, we designed a fluorescence-modified Wt-G4, tested whether G4 was processed by Cas12a to separate from Wt after adding the target, and found that neither ssDNA nor dsDNA binding enabled Cas12a to separate Wt-G4 (Figure 2d,e): this leads further support to the docking results and the hypothesis according to which the presence of a G4 blocks the protein channels of Cas12a, thereby preventing the recognition of its DNA targets.

Development of a Photocontrolled Chimeric CRISPR-G4 System. To further benefit from the G4-mediated control of Cas12a activity, we next developed a novel photoactivatable CRISPR strategy using a photoremovable G4 block. As illustrated in Figure 3a, we used a photocleavable linker (PC-linker) to connect Wt crRNA to G4, the resulting construct being consequently termed Wt-PC-G4 (Table S1). Upon exposure to UV light, the PC-linker is broken and the G4 trigger is removed, which results in an active CRISPR/Cas12a system. We thus evaluated the sensitivity of the PC-linker to irradiation (UV light) and its stability (under sunlight): as seen in Figures S9 and S10, in vitro cleavage experiments showed that 60 s of UV irradiation was sufficient to completely dissociate G4 from crRNA, while the PC-linker remained stable after 4 h of sunlight exposure.

Next, we verified the ability of Wt-PC-G4 to regulate the *cis*-cleavage activity of Cas12a, performing in vitro DNA cleavage experiments: the results seen in Figures 3 and S11 showed that the cleavage efficiency is 94.1% for Wt, 8.4% for Wt-PC-G4 without irradiation, and 93.4% after 60 s of UV irradiation. These results confirmed that this new CRISPR-G4 system can effectively control the *cis*-cleavage activity of Cas12a through light, and the photoregulation of its *trans*-cleavage activity was also demonstrated (Figure 3c). In addition, we found that Wt and UV-treated Wt-PC-G4 showed consistent detection performance of the target DNA (Figure 3d–f). The specificity of this system was then assessed using both Wt and Wt-G4, employing target mutation assays for the detection of target DNA (i.e., with one or two mutated nucleotides, Figures S12, S13, and Table S4): as seen in Figures S14-17, the inhibition efficiency of Wt-G4 is insensitive to mutations, suggesting that

https://doi.org/10.1021/acs.analchem.5c04782
Anal. Chem. 2025, 97, 24634−24642

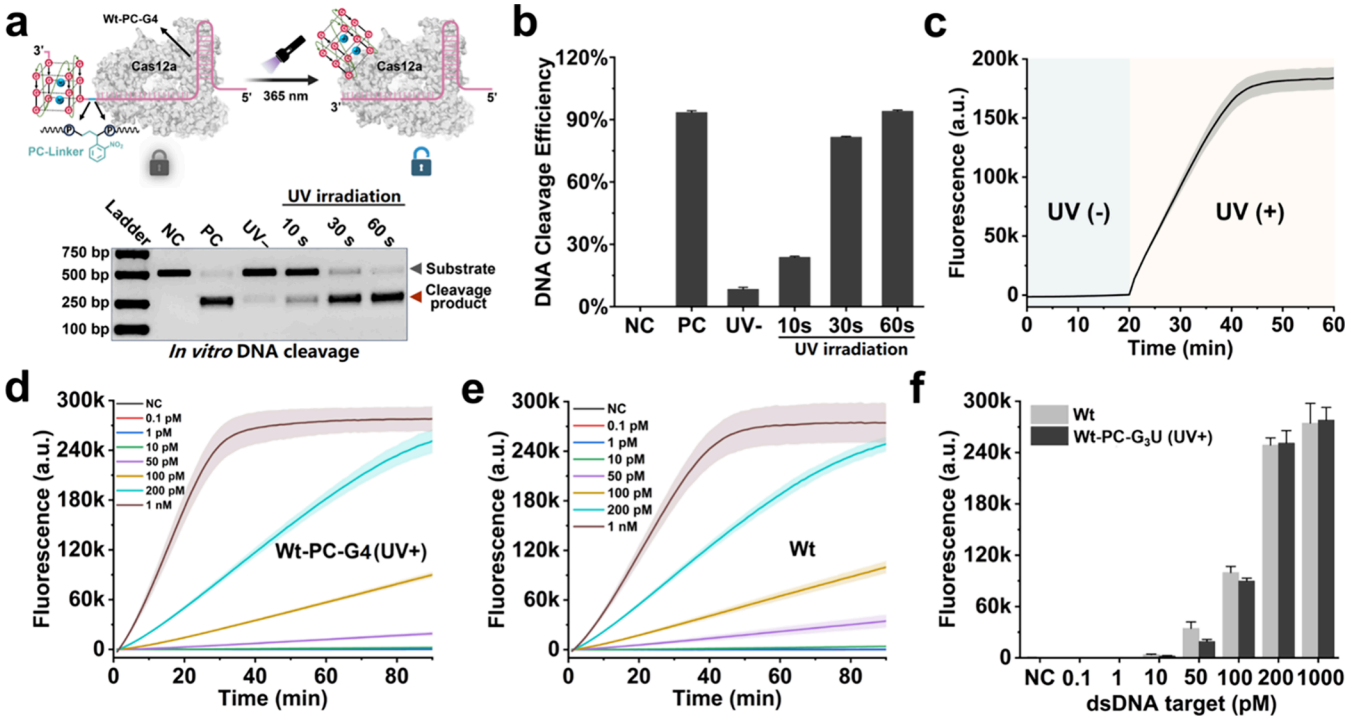

Figure 3. Design of photocontrolled CRISPR regulatory strategy. (a) Schematic representation of the photocontrolled chimeric CRISPR-G4 system and regulation of Cas12a *cis*-cleavage. Negative control (NC) and positive control (PC) indicate no RNP was added and dsDNA template treated with Wt/Cas12a, respectively; "UV-" represents the dsDNA template was treated with Wt-PC-G4/Cas12a without being exposed to UV light. The dsDNA template concentration is 5 nM, the RNP concentration is 65 nM, and the raw data are shown in Figure S11. (b) DNA cleavage efficiency calculated from the gel in panel (a). (c) Photoinitiated *trans*-cleavage of Cas12a. The concentration of ssDNA activator used is 1 nM, and RNP is 10 nM. The reaction is incubated at 37 °C for 20 min and then irradiated with UV lamp (λ = 365 nm, 40 W) for 1 min to activate the CRISPR system. (d, e) Sensitivity analysis of the CRISPR/Cas12a system using UV-treated Wt-PC-G4 (d) or wild crRNA (e) with various concentrations of dsDNA target (RNP was 10 nM). (f) Comparison of fluorescence intensity of the CRISPR/Cas12a system using Wt or UV-treated Wt-PC-G4. Data for (b–f) are presented as mean ± standard deviation (n = 3 technical replicates).

our photocontrolled crRNA-G4 system constitutes a robust and specific CRISPR regulatory strategy.

Exploration of Possible Application of Photocontrolled Chimeric CRISPR-G4 System. To explore the potential application of this photocontrolled CRISPR-G4 system, a RPA step was integrated to make the target detection in a one-pot experiment (Figure 4a): the target DNA is first amplified by RPA in the presence of the inactive Wt-PC-G4 (to avoid interference) and then, the G4 trigger is removed upon UV irradiation allowing the crRNA to specifically recognize the amplicon, so that the fluorescence signal can be monitored by *trans*-cutting the FQ-labeled ssDNA reporter. The practicality of this system was demonstrated with the detection of oncogenetic human papillomavirus 16 (HPV-16): the results seen in Figures 4b and S18 showed that a signal is obtained only when all necessary components are present upon UV irradiation, confirming the reliability of our strategy. Its efficiency was compared to two different methods, the traditional one-pot (RPA and CRISPR detection are performed simultaneously, but the two processes are incompatible) and the two-step (RPA and CRISPR detection in a stepwise manner) assays: as seen in Figure 4c–e, the traditional one-pot method could detect 100 copies/μL of HPV-16 L1 gene at best, while the two-step method and the photoinitiated one-pot assay in this work are approximately 1 copy/μL. Our new strategy provides the same level of sensitivity as the two-step method, while being more practically convenient and straightforward, as it does not necessitate the manipulation of amplicons required in the two-step method.

The sensitivity of this method relies on the rapid accumulation of amplicons during the amplification of HPV-16 targets by RPA (Figure 4f), which are recognized and cleaved by the CRISPR system in the traditional one-pot assay (RPA+Wt), thereby preventing their effective enrichment, while the photoinitiated CRISPR does not interfere with amplicon enrichment. The specificity of this method was also assessed against a series of other viral DNA targets (HPV-6, 18, 33 and 58, SARS-CoV-2, and Mpox virus) and was found to be excellent (Figures 4g and S19). Finally, we showed that crRNA-G4 also improves the stability of RNA, notably against ribonucleases (Figure S20), which is critical for nucleic acid detection in complex media such as those used for point-of-care testing.

Photocontrolled Chimeric CRISPR-G4 System for Pseudovirus Detection and Clinical Diagnosis. The reliability of this system made it suited to be used with real clinical samples: the workflow used, schematically represented in Figure 5a, relies on the extraction of nucleic acid from vaginal swabs before being treated with the photoinitiated CRISPR/Cas12a system. We used two different reading options, the fluorescence for its sensitivity, and lateral flow test strip for its practical convenience. We first confirmed the sensitivity of these readout methods using HPV-16 detection as a model: as seen in Figure 5b–e, the detection of HPV-16 was possible down to 1 copy/μL by fluorescence, and down to

https://doi.org/10.1021/acs.analchem.5c04782
Anal. Chem. 2025, 97, 24634–24642

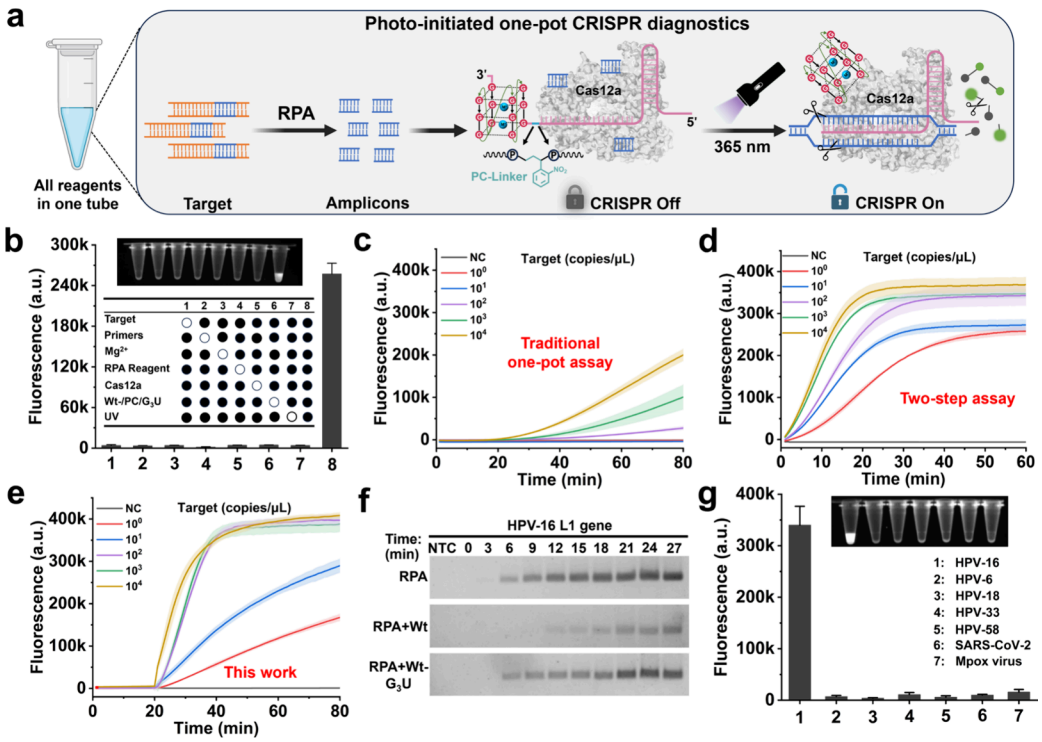

Figure 4. Photocontrolled chimeric CRISPR-G4 system for nucleic acid detection. (a) Schematic of the photoinitiated one-pot CRISPR assay; the target is first amplified by RPA, and at this time, the amplicon cannot be recognized by CRISPR system, and only through the UV light can activate the CRISPR system to produce fluorescent signals. (b) Feasibility of the photoinitiated one-pot assay (the top shows the corresponding image captured under UV light). The concentration of target HPV-16 is 100 fM, and the corresponding raw data are shown in Figure S18. (c–e) Sensitivity analysis of the L1 gene of HPV-16 standard nucleic acids using the traditional one-pot assay (c), two-step assay (d), and this work (e), respectively. (f) Accumulation of RPA amplicons in the one-pot assay. The RPA component, 50 nM RNP, and 100 fM HPV-16 dsDNA are incubated at 37 °C for 0, 3, 6, 9, 12, 15, 18, 21, 24, and 27 min, respectively. The results were analyzed by 1% agarose gels. "NTC" indicates the no-target control test. (g) Specificity of the photoinitiated one-pot assay (the top shows the corresponding image captured under UV light). The target HPV-16 concentration is 100 fM, and the interfering targets are 1 pM. The raw data are shown in Figure S19. Data for parts (b–e) and (g) are presented as mean ± standard deviation (n = 3 technical replicates).

10 copies/μL using strips. Next, we tested 50 clinical samples suspected of an HPV-16 infection. We first tested these samples by qPCR, the gold standard method in clinical testing: with a cycle threshold (Ct) fixed at 38, qPCR investigations showed that 23 samples were HPV-16 positive and 27 negative (Figures 5f, S21 and S22). Quite satisfyingly, the photoinitiated CRISPR/Cas12a system led to 22 positive and 28 negative samples (Figures 5g and S23), with a unique false-negative result (sample 35, Ct = 29.41). The false-negative result for sample 35 is likely due to the extremely low abundance of the target HPV-16 gene, which led to a weak fluorescence signal that did not reach the detection threshold (Figure S23). We believe that increasing the RPA incubation time would enhance the signal response.

The sensitivity of this method was calculated to be 95.7% and its specificity was 100% (Figure 5h), which further highlights its clinical potential. The performance of this system was further assessed by the receiver operating characteristic (ROC) curve analysis (Figure 5i): the area under the curve (AUC) value was 0.978, suggesting strong concordance with the qPCR results. Beyond its efficiency, this system is also faster than qPCR (results are obtained within 25 min versus ca. 1 h for qPCR), and it does not rely on complicated manipulation and/or expensive equipment (such as qPCR instruments), notably when implemented with lateral flow test strips. The integration of the photoinitiated CRISPR system with various readout methods can be used for nucleic acid diagnostics in different scenarios, especially important for point-of-care testing in resource-poor areas. Furthermore, compared with previously reported sensing platforms, our method exhibits significant advantages in terms of turnaround time, analytical sensitivity, and portability (Table S5).

CONCLUSIONS

In this study, we have shown that both the *cis*- and *trans*-cleavage activities of Cas12a could be directly controlled by the introduction of a photoremovable G4 trigger in the 3′ region of crRNA. The reason for the G4-mediated Cas12a inhibition is that the G4 acts as steric barrier that prevents the DNA target from accessing the protein channel of Cas12a, thereby inactivating the whole CRISPR system. We introduced a PC-linker in order to gain control over the CRISPR/Cas12a activity in a spatiotemporal manner, as its activity could be fully restored upon irradiation. This was further exploited designing a one-pot assay which integrates both CRISPR/Cas12a and RPA systems, though RPA is incompatible with CRISPR detection: the photocontrol step was thus used to make this possible and results in the development of a one-pot detection system which is fast, simple, and, above all, efficient. This was demonstrated with the diagnosis of 50 clinical samples for HPV infection: this system turned out to be 95.7% sensitive and 100% specific, which must be added to its rapidity (25 min) and practical convenience (being implementable as lateral flow test strips). Therefore, we believe that

https://doi.org/10.1021/acs.analchem.5c04782
Anal. Chem. 2025, 97, 24634−24642

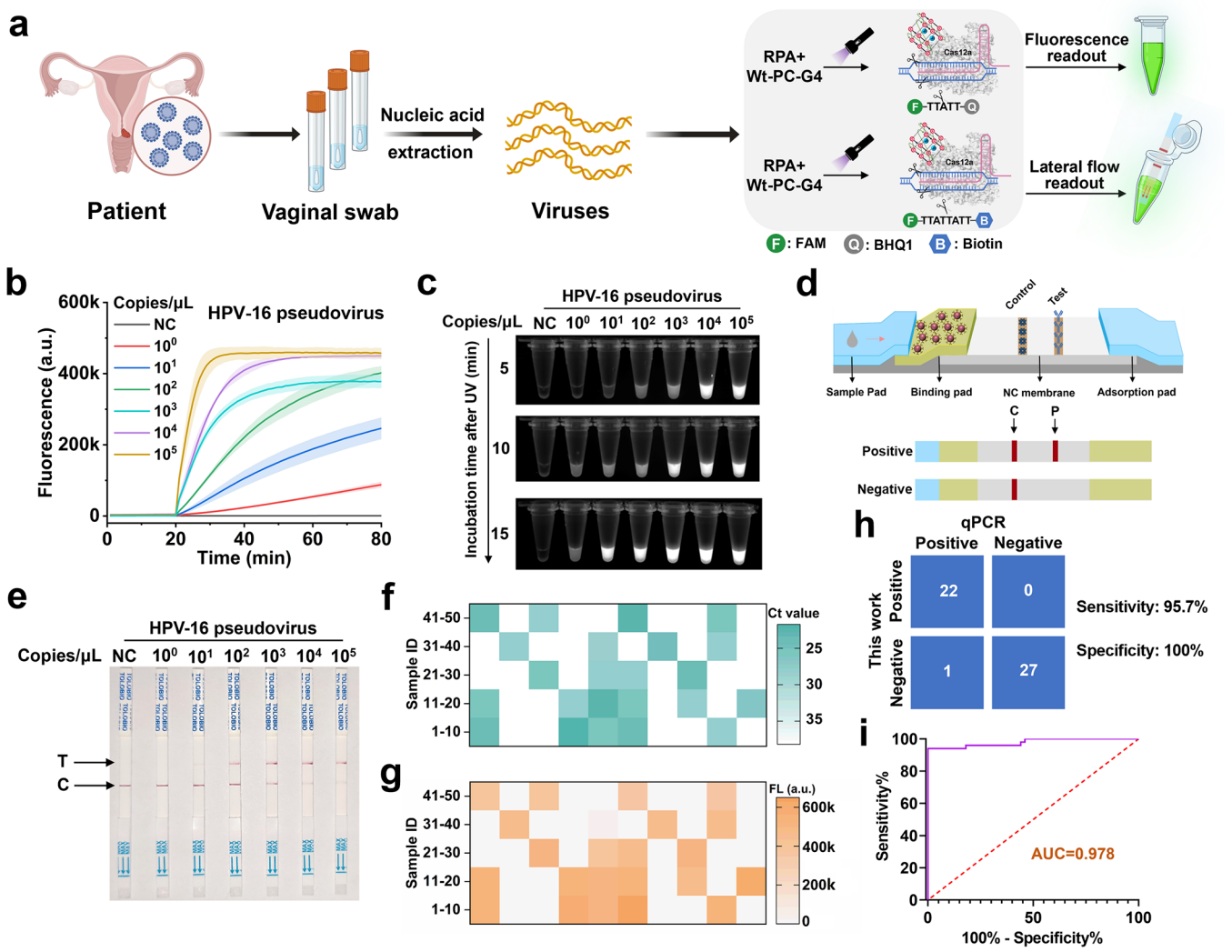

Figure 5. Photoinitiated one-pot CRISPR assay for clinical sample detection. (a) Schematic representation of nucleic acid extraction from the vaginal swab and detection via the light-started one-pot method. The results can be detected using fluorescence or a lateral flow test strip. (b) Sensitivity analysis of the proposed assay (real-time fluorescence) with HPV-16 pseudoviruses. (c) Direct observation of different concentrations of HPV-16 pseudovirus under UV light. The reaction was incubated at 37 °C for 5, 10, and 20 min before imaging under UV light. (d) Principle of the lateral flow test strip. (e) Result of HPV-16 pseudovirus detection with lateral flow test strip. (f) Results from 50 clinical samples tested with the qPCR assay. The color depth in the heatmap represents the magnitude of the Ct values. (g) Results of 50 clinical samples using a light-initiated one-pot CRISPR assay. The color depth in the heatmap indicates the final fluorescence intensity of the reaction. (h) Confusion matrix analysis of 50 clinical samples using this work and qPCR assay. (i) ROC curve of the proposed method for diagnosis of HPV-16 viral infection. The AUC value is calculated using GraphPad Prism 8. Data for (b) are presented as mean ± standard deviation (n = 3 technical replicates).

this photocontrolled CRISPR-G4 system has a great potential for clinical applications but not only, as it could be adapted to other fields (bioimaging, gene expression regulation) straightforwardly. It is noteworthy that several limitations warrant consideration for our findings herein: (*i*) the PC-linker in the photoactivatable crRNA (Wt-PC-G4) is photosensitive. Although we demonstrated that it remains intact under ambient light for several hours, it should be preserved under light-protected conditions; (*ii*) the cost of Wt-PC-G4, which cannot be synthesized via reverse transcription, is higher than that of conventional crRNA; and (*iii*) G4 destabilizers potentially present in complex sample matrices may interfere with G4 formation, thereby reducing the efficiency of this method. Thus, the incorporation of more resistant and affordable blockers should be considered for further developments.

■ ASSOCIATED CONTENT

Supporting Information

The Supporting Information is available free of charge at https://pubs.acs.org/doi/10.1021/acs.analchem.5c04782.

Supplementary methods; DNA and RNA sequences; CD and fluorescence spectra; real-time fluorescence curves; PAGE and agarose electrophoresis images; and clinical sample analysis (PDF)

■ AUTHOR INFORMATION

Corresponding Author

Jun Zhou − *State Key Laboratory of Analytical Chemistry for Life Science, School of Chemistry and Chemical Engineering, Nanjing University, Nanjing 210093, P. R. China;* orcid.org/0000-0002-6793-3169; Email: jun.zhou@nju.edu.cn

https://doi.org/10.1021/acs.analchem.5c04782
Anal. Chem. 2025, 97, 24634−24642

Authors

Xinrong Yan − *State Key Laboratory of Analytical Chemistry for Life Science, School of Chemistry and Chemical Engineering, Nanjing University, Nanjing 210093, P. R. China;* orcid.org/0009-0003-5574-2546

Bin Liu − *State Key Laboratory of Analytical Chemistry for Life Science, School of Chemistry and Chemical Engineering, Nanjing University, Nanjing 210093, P. R. China*

Shuguang Zhou − *Department of Gynecology, Linquan Maternity and Child Healthcare Hospital, Fuyang 236400, P. R. China*

Yanjun Fan − *Department of Gynecology, Linquan Maternity and Child Healthcare Hospital, Fuyang 236400, P. R. China*

Shijiong Wei − *State Key Laboratory of Analytical Chemistry for Life Science, School of Chemistry and Chemical Engineering, Nanjing University, Nanjing 210093, P. R. China*

Dehui Qiu − *State Key Laboratory of Analytical Chemistry for Life Science, School of Chemistry and Chemical Engineering, Nanjing University, Nanjing 210093, P. R. China*

Henglong Xiang − *State Key Laboratory of Analytical Chemistry for Life Science, School of Chemistry and Chemical Engineering, Nanjing University, Nanjing 210093, P. R. China*

Jiahang Zhou − *State Key Laboratory of Analytical Chemistry for Life Science, School of Chemistry and Chemical Engineering, Nanjing University, Nanjing 210093, P. R. China*

Jean-Louis Mergny − *State Key Laboratory of Analytical Chemistry for Life Science, School of Chemistry and Chemical Engineering, Nanjing University, Nanjing 210093, P. R. China; Laboratoire d'Optique et Biosciences (LOB), Ecole Polytechnique, CNRS, INSERM, Institut Polytechnique de Paris, Palaiseau 91120, France;* orcid.org/0000-0003-3043-8401

David Monchaud − *Institut de Chimie Moléculaire de l'Université de Bourgogne (ICMUB), CNRS, UMR6302, Université Bourgogne Europe (UBE), Dijon 21078, France;* orcid.org/0000-0002-3056-9295

Huangxian Ju − *State Key Laboratory of Analytical Chemistry for Life Science, School of Chemistry and Chemical Engineering, Nanjing University, Nanjing 210093, P. R. China;* orcid.org/0000-0002-6741-5302

Complete contact information is available at: https://pubs.acs.org/10.1021/acs.analchem.5c04782

Author Contributions

The manuscript was written through contributions of all authors. All authors have given approval to the final version of the manuscript. X.Y. and B.L. contributed equally to this paper.

Notes

The authors declare no competing financial interest.

■ ACKNOWLEDGMENTS

We gratefully acknowledge the National Natural Science Foundation of China (22374070, 22177047), the State Key Laboratory of Analytical Chemistry for Life Science (5431ZZXM2406), and the Fundamental Research Funds for the Central Universities (202200324, 202200325, and 020514380299).

■ REFERENCES

(1) Weng, Z.; You, Z.; Yang, J.; Mohammad, N.; Lin, M.; Wei, Q.; Gao, X.; Zhang, Y. *Angew. Chem., Int. Ed.* **2023**, *62* (17), No. e202214987.

(2) Pacesa, M.; Pelea, O.; Jinek, M. *Cell* **2024**, *187* (5), 1076−1100.

(3) Yoshimi, K.; Takeshita, K.; Yamayoshi, S.; Shibumura, S.; Yamauchi, Y.; Yamamoto, M.; Yotsuyanagi, H.; Kawaoka, Y.; Mashimo, T. *iScience* **2022**, *25* (2), No. 103830.

(4) Hu, C.; Ni, D.; Nam, K. H.; Majumdar, S.; McLean, J.; Stahlberg, H.; Terns, M. P.; Ke, A. *Mol. Cell* **2022**, *82* (15), 2754−2768.

(5) Hu, T.; Ji, Q.; Ke, X.; Zhou, H.; Zhang, S.; Ma, S.; Yu, C.; Ju, W.; Lu, M.; Lin, Y.; et al. *Commun. Biol.* **2024**, *7* (1), 858.

(6) Pardee, K.; Green, A. A.; Takahashi, M. K.; Braff, D.; Lambert, G.; Lee, J. W.; Ferrante, T.; Ma, D.; Donghia, N.; Fan, M.; et al. *Cell* **2016**, *165* (5), 1255−1266.

(7) Zetsche, B.; Gootenberg, J. S.; Abudayyeh, O. O.; Slaymaker, I. M.; Makarova, K. S.; Essletzbichler, P.; Volz, S. E.; Joung, J.; van der Oost, J.; Regev, A.; et al. *Cell* **2015**, *163* (3), 759−771.

(8) Gootenberg, J. S.; Abudayyeh, O. O.; Lee, J. W.; Essletzbichler, P.; Dy, A. J.; Joung, J.; Verdine, V.; Donghia, N.; Daringer, N. M.; Freije, C. A.; et al. *Science* **2017**, *356* (6336), 438−442.

(9) Harrington, L. B.; Burstein, D.; Chen, J. S.; Paez-Espino, D.; Ma, E.; Witte, I. P.; Cofsky, J. C.; Kyrpides, N. C.; Banfield, J. F.; Doudna, J. A. *Science* **2018**, *362* (6416), 839−842.

(10) Strecker, J.; Jones, S.; Koopal, B.; Schmid-Burgk, J.; Zetsche, B.; Gao, L.; Makarova, K. S.; Koonin, E. V.; Zhang, F. *Nat. Commun.* **2019**, *10* (1), 212.

(11) Li, S.-Y.; Cheng, Q.-X.; Liu, J.-K.; Nie, X.-Q.; Zhao, G.-P.; Wang, J. *Cell Res.* **2018**, *28* (4), 491−493.

(12) Swarts, D. C.; Jinek, M. *Mol. Cell* **2019**, *73* (3), 589−600.

(13) Kaminski, M. M.; Abudayyeh, O. O.; Gootenberg, J. S.; Zhang, F.; Collins, J. J. *Nat. Biomed. Eng.* **2021**, *5* (7), 643−656.

(14) Li, H.; Xie, Y.; Chen, F.; Bai, H.; Xiu, L.; Zhou, X.; Guo, X.; Hu, Q.; Yin, K. *Chem. Soc. Rev.* **2023**, *52* (1), 361−382.

(15) Ramachandran, A.; Huyke, D. A.; Sharma, E.; Sahoo, M. K.; Huang, C.; Banaei, N.; Pinsky, B. A.; Santiago, J. G. *Proc. Natl. Acad. Sci. U. S. A.* **2020**, *117* (47), 29518−29525.

(16) Samanta, D.; Ebrahimi, S. B.; Ramani, N.; Mirkin, C. A. *J. Am. Chem. Soc.* **2022**, *144* (36), 16310−16315.

(17) Dai, Y.; Somoza, R. A.; Wang, L.; Welter, J. F.; Li, Y.; Caplan, A. I.; Liu, C. C. *Angew. Chem., Int. Ed.* **2019**, *58* (48), 17399−17405.

(18) Li, S.-Y.; Cheng, Q.-X.; Wang, J.-M.; Li, X.-Y.; Zhang, Z.-L.; Gao, S.; Cao, R.-B.; Zhao, G.-P.; Wang, J. *Cell Discovery* **2018**, *4* (1), 20.

(19) Ye, X.; Wu, H.; Liu, J.; Xiang, J.; Feng, Y.; Liu, Q. *Trends Biotechnol.* **2024**, *42* (11), 1410−1426.

(20) Joung, J.; Ladha, A.; Saito, M.; Kim, N.-G.; Woolley, A. E.; Segel, M.; Barretto, R. P. J.; Ranu, A.; Macrae, R. K.; Faure, G.; et al. *N. Engl. J. Med.* **2020**, *383* (15), 1492−1494.

(21) Chen, L.; Hu, M.; Zhou, X. *Trends Biotechnol.* **2025**, *43* (1), 98−110.

(22) Liu, X.; Zhou, E.; Qi, Q.; Xiong, W.; Tian, T.; Zhou, X. *Acc. Chem. Res.* **2025**, *58* (8), 1262−1274.

(23) Zhang, W.; Zhong, Y.; Wang, J.; Zou, G.; Chen, Q.; Liu, C. *Nucleic Acids Res.* **2025**, *53* (3), No. gkaf040.

(24) Ma, L.; Lu, M.; Jia, J.; Wang, N.; Li, Y.; Peng, W.; Man, S. *Trends Biotechnol.* **2025**, *43* (1), 8−11.

(25) Cao, L.; Wang, Z.; Lei, C.; Nie, Z. *Anal. Chem.* **2025**, *97* (11), 5866−5879.

(26) Jain, P. K.; Ramanan, V.; Schepers, A. G.; Dalvie, N. S.; Panda, A.; Fleming, H. E.; Bhatia, S. N. *Angew. Chem., Int. Ed.* **2016**, *55* (40), 12440−12444.

(27) Hu, M.; Qiu, Z.; Bi, Z.; Tian, T.; Jiang, Y.; Zhou, X. *Proc. Natl. Acad. Sci. U. S. A.* **2022**, *119* (26), No. e2202034119.

(28) Qi, Q.; Liu, X.; Xiong, W.; Zhang, K.; Shen, W.; Zhang, Y.; Xu, X.; Zhong, C.; Zhang, Y.; Tian, T.; Zhou, X. *Cell Chem. Biol.* **2024**, *31* (10), 1839−1851.

(29) Liu, P.; Lin, Y.; Zhuo, X.; Zeng, J.; Chen, B.; Zou, Z.; Liu, G.; Xiong, E.; Yang, R. *Angew. Chem., Int. Ed.* **2024**, *63* (23), No. e202401486.
(30) Carlson-Stevermer, J.; Kelso, R.; Kadina, A.; Joshi, S.; Rossi, N.; Walker, J.; Stoner, R.; Maures, T. *Nat. Commun.* **2020**, *11* (1), 5041.
(31) Hu, M.; Liu, R.; Qiu, Z.; Cao, F.; Tian, T.; Lu, Y.; Jiang, Y.; Zhou, X. *Angew. Chem., Int. Ed.* **2023**, *62* (23), No. e202300663.
(32) Moroz-Omori, E. V.; Satyapertiwi, D.; Ramel, M.-C.; Høgset, H.; Sunyovszki, I. K.; Liu, Z.; Wojciechowski, J. P.; Zhang, Y.; Grigsby, C. L.; Brito, L.; et al. *ACS Cent. Sci.* **2020**, *6* (5), 695−703.
(33) Zhou, W.; Brown, W.; Bardhan, A.; Delaney, M.; Ilk, A. S.; Rauen, R. R.; Kahn, S. I.; Tsang, M.; Deiters, A. *Angew. Chem., Int. Ed.* **2020**, *59* (23), 8998−9003.
(34) Lu, S.; Tong, X.; Han, Y.; Zhang, K.; Zhang, Y.; Chen, Q.; Duan, J.; Lei, X.; Huang, M.; Qiu, Y.; et al. *Nat. Biomed. Eng.* **2022**, *6* (3), 286−297.
(35) Cheng, Z.-H.; Luo, X.-Y.; Yu, S.-S.; Min, D.; Zhang, S.-X.; Li, X.-F.; Chen, J.-J.; Liu, D.-F.; Yu, H.-Q. *Nat. Commun.* **2025**, *16* (1), 1166.
(36) Huppert, J. L. *Chem. Soc. Rev.* **2008**, *37* (7), 1375−1384.
(37) Mergny, J.-L.; Sen, D. *Chem. Rev.* **2019**, *119* (10), 6290−6325.
(38) Zhang, X.; Dhir, S.; Melidis, L.; Chen, Y.; Yu, Z.; Simeone, A.; Spiegel, J.; Adhikari, S.; Balasubramanian, S. *Nat. Chem.* **2025**, *17* (6), 875−882.
(39) Hänsel-Hertsch, R.; Di Antonio, M.; Balasubramanian, S. *Nat. Rev. Mol. Cell Biol.* **2017**, *18* (5), 279−284.
(40) Deng, H.; Xu, H.; Wang, Y.; Jia, R.; Ma, X.; Feng, Y.; Chen, H. *Nucleic Acids Res.* **2023**, *51* (8), 4064−4077.
(41) Liu, X.; Cui, S.; Qi, Q.; Lei, H.; Zhang, Y.; Shen, W.; Fu, F.; Tian, T.; Zhou, X. *Nucleic Acids Res.* **2022**, *50* (19), 11387−11400.
(42) Huang, W.; Wang, J.; Wang, C.; Liu, Y.; Li, W.; Chen, Q.; Zhai, J.; Xiang, Z.; Liu, C. *Adv. Sci.* **2025**, *12* (7), No. 2411305.
(43) Goldberg, D. C.; Fones, L.; Vivinetto, A. L.; Caufield, J. T.; Ratan, R. R.; Cave, J. W. *ACS Chem. Neurosci.* **2020**, *11* (10), 1504−1518.
(44) Qin, G.; Liu, Z.; Yang, J.; Liao, X.; Zhao, C.; Ren, J.; Qu, X. *Nat. Cell Biol.* **2024**, *26* (7), 1212−1224.
(45) Chen, J.; Lin, X.; Xiang, W.; Chen, Y.; Zhao, Y.; Huang, L.; Liu, L. *Nucleic Acids Res.* **2025**, *53* (3), No. gkae1241.
(46) Abramson, J.; Adler, J.; Dunger, J.; Evans, R.; Green, T.; Pritzel, A.; Ronneberger, O.; Willmore, L.; Ballard, A. J.; Bambrick, J.; et al. *Nature* **2024**, *630* (8016), 493−500.
(47) Banco, M. T.; Ferré-D'Amaré, A. R. *RNA* **2021**, *27* (4), 390−402.
(48) Zhang, D.-H.; Fujimoto, T.; Saxena, S.; Yu, H.-Q.; Miyoshi, D.; Sugimoto, N. *Biochemistry* **2010**, *49* (21), 4554−4563.

https://doi.org/10.1021/acs.analchem.5c04782
Anal. Chem. 2025, 97, 24634−24642